DOI: 10.1002/ejoc.201100818

Fluorescence Properties of 5-(5,6-Dimethoxybenzothiazol-2-yl)-2′-deoxyuridine ($d^{bt}U$) and Oligodeoxyribonucleotides Containing $d^{bt}U$

Wataru Hirose,[a] Kousuke Sato,[a] and Akira Matsuda*[a]

Keywords: Nucleosides / DNA / Fluorescent probes / DNA damage

We describe the synthesis and photophysical properties of 11 substituted 5-(benzothiazol-2-yl)-2′-deoxyuridine derivatives and oligodeoxyribonucleotides (ODNs) containing 5-(5,6-dimethoxybenzothiazol-2-yl)-2′-deoxyuridine ($d^{bt}U$), which was the strongest fluorescent derivative among those prepared. The fluorescence properties of $d^{bt}U$ itself and ODNs containing $d^{bt}U$ show the same tendency of being weaker in both neutral and acidic solution and stronger in basic solution. The ODNs (15mer) containing 16 combinations of 5′-X^{bt}U-3′ and 5′-^{bt}UY-3′, where X, Y = A, T, G, or C, were synthesized, and their fluorescence intensity and quantum yield in basic solution were compared. On average, only the ODN with the 5′-G^{bt}U-3′ sequence shows a 7.9-fold lower fluorescence intensity than the other sequences. Ab initio calculations of 5′-G^{bt}U-3′ and 5′-^{bt}UG-3′ as models under basic conditions suggest that the lower fluorescence of the ODN containing the 5′-G^{bt}U-3′ sequence is caused by a wider overlap between stacked guanine (Gua) and ^{bt}Ura than that of the 5′-^{bt}UG-3′ sequence and that the HOMO is delocalized not only on ^{bt}Ura but also on Gua.

Introduction

DNA in living cells is continuously damaged by reactive oxygen species derived from UV, ionizing radiation and cellular respiration. The oxidative lesion in DNA has been implicated in mutagenesis, carcinogenesis, and aging.[1] Various oxidative base lesions (≈50 known adducts) have been reported,[2] and 8-oxoguanine is considered to be one of the most abundant oxidative base lesions.[3] Base pairing, mutagenicity, repair and detection of 8-oxoguanine have all been extensively investigated.[4] On the other hand, 5-formyluracil (^{fo}Ura) is one of the oxidized thymine-lesions and known to be generated in yields comparable to that of 8-oxoguanine in γ-irradiated DNA.[5] DNA polymerization across ^{fo}Ura in vitro with the *E. coli* Pol I Klenow fragment introduces guanine (Gua) as well as adenine (Ade) in DNA.[6] Zhang et al. reported that dCTP as well as dATP are frequently incorporated but only a small amount of dGTP is incorporated into the site opposite to ^{fo}Ura in DNA by the Klenow fragment (*exo*–).[7] These misincorporations induce mutation (from A:T to G:C and A:T to C:G) by mispairing between an ionized form of ^{fo}Ura and Gua or between ^{fo}Ura and Cyt during DNA replication. Experiments with Chinese hamster fibroblast cells indicate that 5-formyl-2′-deoxyuridine ($d^{fo}U$) is more mutagenic in mammalian cells than in bacteria,[8] and ^{fo}Ura incorporated into DNA causes induction of A:T to C:G and A:T to T:A transversions in mammalian cells.[9] It appears that the formation of $d^{fo}U$ and its nucleotides in cells and their subsequent incorporation into DNA and/or the generation of ^{fo}Ura in DNA cause carcinogenicity and/or aging cells. Therefore, a selective and sensitive method for detecting ^{fo}Ura in DNA would be highly useful since the existing methods have complicated protocols. Moreover, a long time is required for analysis by HPLC and/or mass spectroscopy following complete enzymatic hydrolysis of the target DNA to its corresponding nucleosides and isotopically labeled $d^{fo}U$ (^{13}C and/or ^{15}N) as an internal standard is needed.[10]

Some selective detection methods for DNA damage by chemical reagents have recently been reported.[11] However, trace amounts of excess fluorescent and/or colorimetric probe remain even after extensive washing, which interfere with the analysis by giving higher background signals. We recently reported a new concept for simple ^{fo}Ura detection in DNA using a fluorogenic reagent, 2-amino-4,5-dimethoxythiophenol, which has no fluorescence before reaction with the target ^{fo}Ura in DNA.[12] After reaction with $d^{fo}U$, the formyl group at the 5-position of the uracil moiety is smoothly converted into a benzothiazol-2-yl group conjugated with a uracil ring, which exhibits good fluorescence as does 5-furyl-2′-deoxyuridine.[13] Therefore, ^{fo}Ura in DNA is directly detected by fluorescence measurements without enzymatic hydrolysis of the target DNA to its corresponding nucleosides, HPLC separation, and by mass spectroscopic detection.

In this work, we synthesized 10 more substituted 5-(benzothiazol-2-yl)-2′-deoxyuridine derivatives and characterized their photophysical properties in order to investigate substituent effects on the benzothiazole ring. The fluores-

[a] Faculty of Pharmaceutical Sciences, Hokkaido University, Kita-12, Nishi-6, Kita-ku, Sapporo 060-0812, Japan
Fax: +81-11-706-4980
E-mail: matuda@pharm.hokudai.ac.jp

Supporting information for this article is available on the WWW under http://dx.doi.org/10.1002/ejoc.201100818.

cence properties and structural characteristics of oligodeoxyribonucleotides (ODNs) containing 5-(5,6-dimethoxybenzothiazol-2-yl)-2′-deoxyuridine ($d^{bt}U$), the strongest fluorescent derivative among the derivatives prepared, were investigated. We found that $d^{bt}U$ causes only minor structural perturbations to the natural B-form DNA. Furthermore, the quantum yields of the ODNs containing $d^{bt}U$ are high with the exception of the ODNs having a 5′-neighboring guanine in the sequence. Moreover, we investigated the quenching effect of the 5′-G sequence by modeling and molecular orbital (MO) calculations. Finally, $d^{bt}U$ was found to be a very promising new fluorescent analogue for detecting ^{fo}Ura in DNA while showing low sensitivity to its microenvironment.

Results and Discussion

Synthesis and Photophysical Properties of the 5-(Benzothiazol-2-yl)-2′-deoxyuridine Derivatives

In order to study how the fluorescence might be influenced by substituents on the benzothiazole ring, 11 substituted 5-(benzothiazol-2-yl)-2′-deoxyuridine derivatives were synthesized (Scheme 1). The aniline derivatives **1b**–**l** were thiocyanated by bromine and ammonium thiocyanate to afford the 2-aminobenzothiazole derivatives **2b**–**l**. Compounds **2a**–**l** were then hydrolyzed with aqueous KOH in ethylene glycol under reflux to afford the 2-aminothiophenol derivatives **3′a**–**l**, which were obtained as the disulfides **3a**–**l** after O_2 oxidation. The disulfides **3a**–**l** were used for the reactions with $d^{fo}U$ after reduction in situ to **3′a**–**l** by dithiothreitol (DTT). The formyl group at the 5-position of the uracil was smoothly converted to a benzothiazoline derivative after addition of the aminothiophenol derivative **3′** to $d^{fo}U$ in DMF at room temperature. This compound was easily oxidized to the benzothiazole derivative **4** by addition of H_2O_2 and $Sc(OTf)_3$ at room temperature. The 2-aminothiophenol derivatives **3′a** and **3′c**–**l** reacted smoothly with $d^{fo}U$ to give the desired benzothiazole derivatives **4a** and **4c**–**l**. However, the nitro derivative **3′b** did not react with $d^{fo}U$ under the above conditions.

We then measured the UV absorption and fluorescence spectra of the above 11 benzothiazoles (**4a**, **4c**–**l**) in acidic (A; aqueous 100 mM HCl), neutral (N; 10 mM phosphate buffer, pH 7.0) and basic (B; aqueous 100 mM NaOH) solutions for comparison of their fluorescence properties (Table 1), and their spectra are shown in the Figure S1. Generally, when the pH of the solution is changed, the fluorescence of **4** also changes, and most compounds show higher quantum yields in basic solution than in either acidic or neutral solutions. This was especially evident in the case of 5-(6-methoxybenzothiazol-2-yl)-2′-deoxyuridine (**4h**) and 5-(5,6-dimethoxybenzothiazol-2-yl)-2′-deoxyuridine (**4i**, $d^{bt}U$), which have high quantum yields of 0.601 and 0.701 and a brightness of 10600 and 14000, respectively. These values are excellent for fluorescent compounds in aqueous solution.[14] However, in the case of **4**, it was difficult to see any relationship between the substituent effects and the

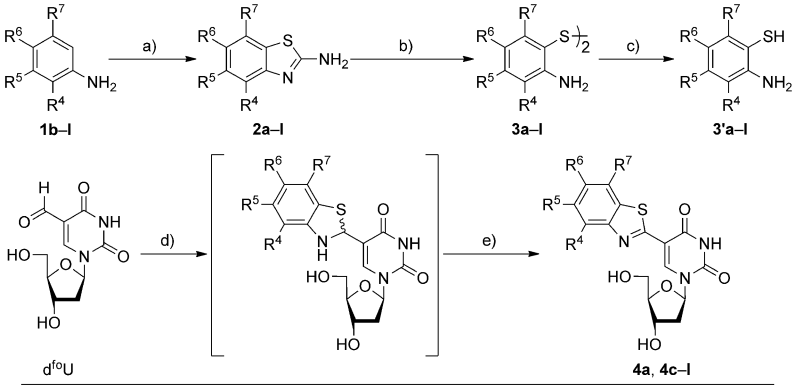

compound	R^4	R^5	R^6	R^7	**2** (yield, %)	**3** (yield, %)	**4** (yield, %)
a	H	H	H	H	**2a** [a]	**3a** (61)	**4a** (82)
b	H	H	NO_2	H	**2b** (15)	**3b** (63)	N.R.[c]
c	H	H	F	H	**2c** (71)	**3c** (92)	**4c** (69)
d	H	H	Cl	H	**2d** (79)	**3d** (79)	**4d** (92)
e	H	H	Br	H	**2e** (71)	**3e** (68)	**4e** (97)
f	H	H	I	H	**2f** (30)	**3f** (49)	**4f** (66)
g	H	H	Et	H	**2g** (76)	**3g** (68)	**4g** (59)
h	H	H	OMe	H	**2h** (75)	**3h** (74)	**4h** (82)
i	H	OMe	OMe	H	**2i** (78)	**3i** (82)	**4i** (75)
j	OMe	H	OMe	H	**2j** (28)	**3j** (50)	**4j** (67)
k	H	OMe	OMe	OMe	**2k** (47)	**3k** (77)	**4k** (98)
l	H	H	AcNH	H	**2l** (88)	**3l** ($R^6 = NH_2$, n.d.[b])	**4l** (21)

[a] **2a** was purchased. [b] n.d. = not determined. [c] N.R. = no reaction.

Scheme 1. Reagents: (a) Br_2, NH_4SCN, AcOH, 10 °C; (b) aq. KOH, ethylene glycol, reflux; (c) (±)-DTT, DMF; (d) **3′a**–**l**, DMF; (e) aq. H_2O_2, $Sc(OTf)_3$.

fluorescence properties. Since the fluorescence of **4i** in basic solution was found to be the most suitable among the various substituted benzothiazole derivatives (**4a**, **4c**–**l**), we used **4i** for the detection of the oxidative lesion product, ^{fo}Ura, in DNA as previously reported.[12]

Table 1. Fluorescence properties of 5-benzothiazol-2-yl-2′-deoxyuridine derivatives (**4a**, **4c**–**l**).

	solvent	λ_{max}^{abs} [nm]	ε_{max} [M^{-1}cm^{-1}]	λ_{max}^{flu} [nm]	Stokes shift [nm]	Φ	brightness $\Phi \times \varepsilon_{max}$
 **4a**	A[a]	335	14700	416	81	0.067	1000
	N[b]	324	14800	417	93	0.059	900
	B[c]	325	17600	404	79	0.043	800
 **4c**	A	329	17400	418	89	0.100	1700
	N	326	17700	418	92	0.079	1400
	B	326	19700	404	78	0.053	1000
 **4d**	A	331	6100	421	90	0.204	1200
	N	330	6500	420	90	0.173	1100
	B	330	19000	411	81	0.449	8500
 **4e**	A	333	16300	420	87	0.068	1100
	N	330	16500	418	88	0.116	1900
	B	331	20300	406	75	0.100	2000
 **4f**	A	332	10100	423, 457	91, 125	0.030	300
	N	332	10000	420, 457	88, 125	0.031	300
	B	332	24000	408	76	0.030	700
 **4g**	A	345	9100	459	114	0.129	1200
	N	331	8300	461	130	0.172	1400
	B	332	15600	411	79	0.145	2300
 **4h**	A	351	14300	492	141	0.274	3900
	N	336	14600	481	145	0.130	1900
	B	335	17600	424, 456	89, 121	0.601	10600
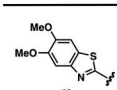 **4i**	A	368	15900	514	146	0.160	2500
	N	351	16600	467	116	0.074	1200
	B	345	20000	458	113	0.701	14000
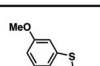 **4j**	A	345	12900	529	184	0.015	200
	N	341	12000	484	143	0.039	500
	B	339	15500	478	139	0.345	5300
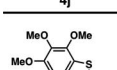 **4k**	A	347	15800	439	92	< 0.001	< 100
	N	343	16100	500	157	0.005	< 100
	B	341	19300	494	153	0.026	500
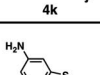 **4l**	A	325	18800	406	81	0.002	< 100
	N	349	12800	512	163	0.004	< 100
	B	346	16100	527	181	0.022	400

[a] A = aq. 100 mM HCl. [b] N = 10 mM phosphate buffer (pH 7.0). [c] B = aq. 100 mM NaOH.

Synthesis of ODNs Containing d^{bt}U

5-(5,6-Dimethoxybenzothiazol-2-yl)-2′-deoxyuridine (**4i**: d^{bt}U) was protected with a DMTr group to afford **5**, which was converted into its phosphoramidite **6** by the conventional method (Scheme 2). The synthesis of ODN was carried out by using a DNA synthesizer model 3400 (ABI) with standard reagents and programs except for a 15-min coupling time for the incorporation of d^{bt}U. The coupling yields were similar to those for the natural DNA synthesis. These ODNs (Figures S2 and S3) were used for fluorescence experiments.

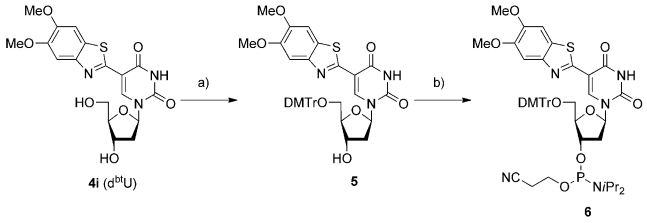

Scheme 2. Reagents: (a) DMTrCl, pyridine, 40 °C, 74%; (b) 2-cyanoethyl *N*,*N*-diisopropylchlorophosphoramidite, *i*Pr_2NEt, CH_2Cl_2, 80%.

Fluorescence Properties of Single-Strand ODNs Containing d^{bt}U

The fluorescence spectra of d^{bt}U were measured in various pH solutions. A much weaker fluorescence was observed in both neutral and acidic solutions, and a much stronger fluorescence was obtained in aqueous 100 mM NaOH. These results suggest that deprotonation of the N3 proton in the uracil moiety contributes to its strong fluorescence. The fluorescence spectra of d^{bt}U and 5′-GACTCAA^{bt}UAGCCGTA-3′ (ODN-A^{bt}UA) are shown in Figure 1. The strong, blue-shifted fluorescence was observed in aqueous 100 mM NaOH at 458 nm (excitation at 350 nm) with a Stokes shift of 108 nm and weaker fluorescence in neutral solution at 490 nm (excitation at 363 nm) in both cases. The fluorescence intensity of ODN-A^{bt}UA is 5.0-fold stronger than d^{bt}U itself in neutral solution, but slightly weaker than d^{bt}U in basic solution. These results reveal that the fluorescence properties of d^{bt}U are maintained even in the ODNs.

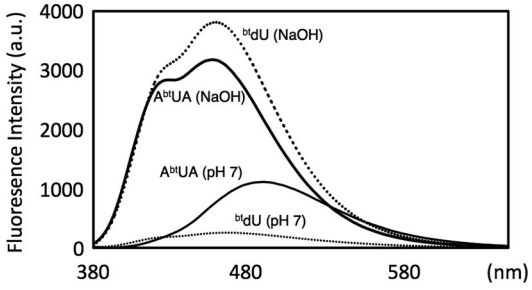

Figure 1. Fluorescence spectra of single-stranded ODN-A^{bt}UA in 10 mM phosphate buffer (pH 7.0) and in aqueous 100 mM NaOH and of d^{bt}U in 10 mM phosphate buffer (pH 7.0) and in aqueous 100 mM NaOH (1.0 μM each). Fluorescence spectra were measured at 25 °C in a 1-cm path length cell by using excitation at 363 nm (in neutral solution) and at 350 nm (in basic solution).

CD Spectra of the Duplex ODN Containing d^{bt}U

CD spectra of the modified duplex ODN-A^{bt}UA:ODN-TAT and the unmodified duplex ODN-ATA:ODN-TAT

(Figures S2 and S4) show a positive CD band at around 280 nm and a negative CD band at 245 nm, the shapes of which are almost the same as that of the unmodified B-form DNA duplex, although the intensity of each band is different (Figure 2). Therefore, these duplexes have a global structure similar to that of the B-form DNA duplex with the Watson–Crick-type base pairing ^{bt}U:A. We next investigated whether the fluorescence spectrum of d^{bt}U changes in the B-form duplex structures.

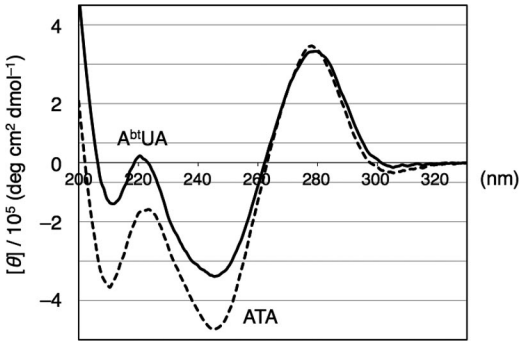

Figure 2. CD spectra of duplexes ODN-ATA:ODN-TAT (dashed) and ODN-A^{bt}UA:ODN-TAT (solid) (3.0 μM each) in 10 mM phosphate buffer (pH 7.0), 150 mM NaCl at 25 °C. Sequences of A^{bt}UA are shown in Figure S2.

Fluorescence Properties of Double-Stranded ODNs Containing d^{bt}U

The fluorescence properties of double-stranded DNA containing d^{bt}U, which consists of the modified ODN-A^{bt}UA with matched complementary DNA (ODN-TAT), are shown in Figure 3. The emission maximum of the modified duplex (490 nm) is slightly shifted relative to those of d^{bt}U itself (467 nm, Figure 1 pH 7) and of the single-stranded ODN-A^{bt}UA in neutral solution [Figure 3, ds (pH 7), dashed]. The fluorescence spectra of the mismatched duplexes are also shown in Figure S5. The dC- and dT-mismatched duplex ODNs (ODN-TCT and ODN-TTT) have stronger fluorescence than the dA-matched ODN-TAT duplex, while the dG-mismatched ODN (ODN-TGT) has the weakest fluorescence among the matched and mismatched duplex ODNs tested. These results indicate that the fluorescence of d^{bt}U in single- or double-stranded ODN is not very different; however, it is slightly affected by the microenvironmental changes in the opposite sequences.

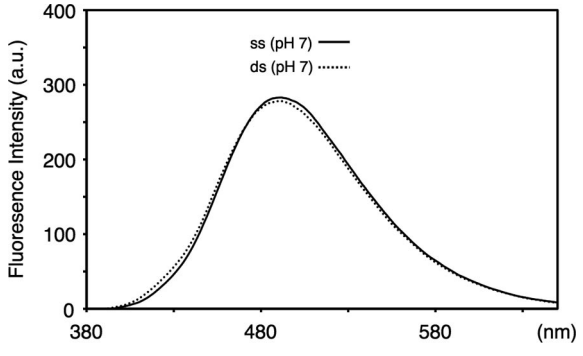

Figure 3. Fluorescence spectra of single- and double-stranded ODN-A^{bt}UA in 10 mM phosphate buffer (pH 7.0) containing 150 mM NaCl (in neutral solution) (0.25 μM each); single strand (solid), double strand (dashed). Fluorescence spectra were measured at 25 °C in a 1-cm path length cell by using excitation at 363 nm (in neutral solution).

5′- and 3′-Neighboring Sequences Influence the Fluorescence Properties of ODNs Containing d^{bt}U

As described above, the fluorescence intensities of the double-stranded DNA containing d^{bt}U are only slightly influenced by the microenvironmental changes in the opposite sequence. Therefore, we then examined the effect of the 5′- and 3′-neighboring sequences of d^{bt}U. The 15mer ODNs containing 16 combinations of neighboring sequences were synthesized (Figure S2), and the fluorescence intensity and quantum yields in neutral and basic solutions were compared (Figures 4 and S6). All the sequences show a lower fluorescence intensity at 490 nm (excited at 363 nm) and a redshift in neutral solution relative to those in basic solution. The quantum yield in Figure S6 also indicates a lower fluorescence in neutral solution and a higher fluorescence in basic solution. This tendency is virtually the same as that of d^{bt}U and ODN-A^{bt}UA. However, the fluorescence of the 5′-G sequences in basic solution (5′-G^{bt}UY-3′, Y = A, G, C, T, Figure 4B) has a 7.9-fold lower intensity on average within the 5′- and 3′-neighboring sequences, although those of the 3′-G sequences (5′-X^{bt}UG-3′, X = A, G, C, T) do not. It is well known that a guanine base quenches the fluorescence of some fluorophores. The dependence of fluorescence quenching on the distance between a dye and a guanine base has been intensively studied by using fluorophores such as acridine, stilbene, and pyrene.[15] However, our sequence-dependent quenching of the fluorescence of d^{bt}U by a neighboring guanine base cannot be explained by only the distance between the dye and the guanine base. Therefore, we investigated the reasons for the lower fluorescence of the 5′-G sequence under basic conditions by computational chemistry.

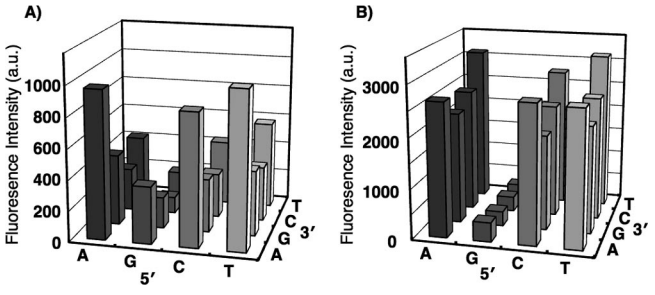

Figure 4. Fluorescence intensity of ODN-X^{bt}UY (1.0 μM); (A) intensity at 490 nm in 10 mM phosphate buffer (pH 7.0, λ_{ex}; 363 nm); (B) intensity at 460 nm in aqueous 100 mM NaOH (λ_{ex}; 350 nm).

The 5′-Neighboring G Sequence Influences on the HOMO and LUMO of d^{bt}U in DNA

Ab initio molecular orbital calculations of stacked bases in DNA were performed with 5′- and 3′-neighboring natural bases in order to elucidate the origin of the remarkable lower fluorescence of 5′-G^{bt}U-3′. In Figure 5, models of the 5′-G^{bt}U-3′ and 5′-^{bt}UG-3′ sequences of the B-form DNA are shown. In this case, the overlapping area of the bases in 5′-G^{bt}U-3′ is greater than that in 5′-^{bt}UG-3′. Theoretical calculations of tautomerism, ionization potential, and the molecular orbitals of the bases in DNA have been widely investigated.[16] Saito et al. have reported that the HOMO of the stacked 5′-GG-3′ sequence is localized mainly on 5′-G in B-form DNA, and base stacking is an important factor for the lowering of the HOMO energy.[17] From these results, 5′-G, which has a greater stacking effect with 3′-^{bt}U, may have a different localization of the HOMO in the dinucleotide model from 3′-G and 5′-^{bt}U. In order to determine the nature of the HOMO and LUMO in a stacked geometry of the duplexes, we carried out ab initio calculations on stacked 5′-X^{bt}U-3′ and 5′-^{bt}UY-3′ (X, Y = A, G,

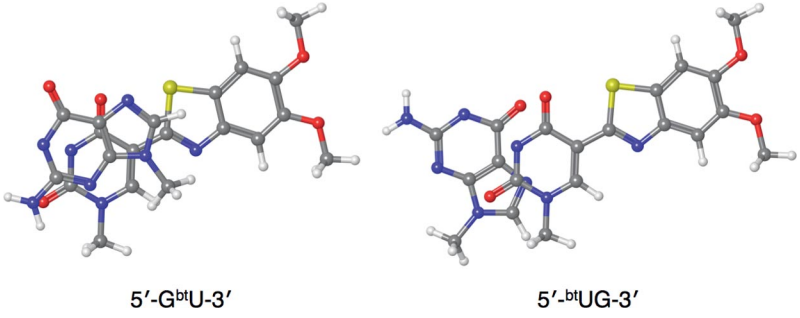

Figure 5. Nucleobase stacking models of the 5′-G^{bt}U-3′ (left) and 5′-^{bt}UG-3′ (right) sequences in B-form DNA. Carbon (gray), hydrogen (white), nitrogen (blue), oxygen (red), and sulfur (yellow).

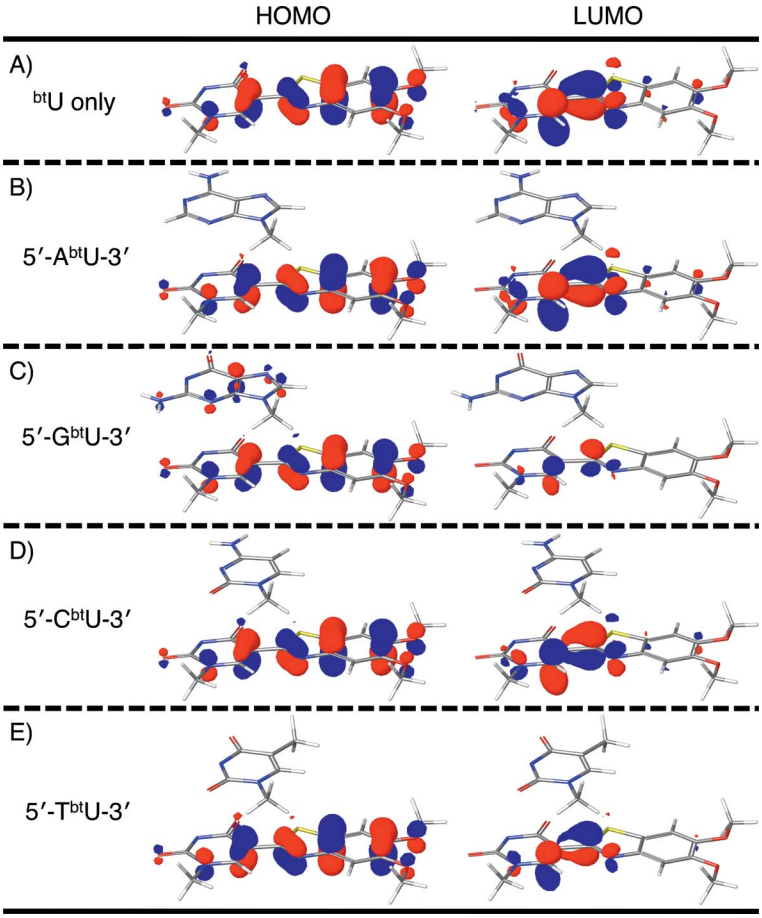

Figure 6. HOMO and LUMO localization of stacked 5′-X^{bt}U-3′ in B-form DNA; (A) ^{bt}Ura only; (B) 5′-A^{bt}U-3′; (C) 5′-G^{bt}U-3′; (D) 5′-C^{bt}U-3′; (E) 5′-T^{bt}U-3′.

C and T). Ab initio calculations were performed by using deprotonated forms of ^{bt}Ura, Gua and Thy at the N3, N1 and N3 positions, respectively, for estimation of the HOMO and LUMO levels under basic conditions. First, the HOMO and LUMO of ^{bt}Ura were calculated as shown in Figure 6A. The HOMO is localized on the benzothiazole ring, and the LUMO is mainly localized on the uracil ring. This result suggests that the fluorescence of d^{bt}U occurs by intramolecular charge transfer (ICT) from the benzothiazole ring to the uracil ring by excitation. The HOMOs and LUMOs of 5′-X^{bt}U-3′ are shown in Figure 6B–E. The HOMOs of 5′-A^{bt}U-3′, 5′-C^{bt}U-3′, and 5′-T^{bt}U-3′ show essentially the same shape, area, and distribution, and the LUMOs of 5′-A^{bt}U-3′, 5′-C^{bt}U-3′, and 5′-T^{bt}U-3′ also appears to have the same shape and distribution. The areas covered by the LUMOs of 5′-C^{bt}U-3′ and 5′-T^{bt}U-3′ are slightly smaller than that of 5′-A^{bt}U-3′. The HOMO of 5′-G^{bt}U-3′ is localized not only on 3′-^{bt}U but also on 5′-G, and the LUMO is much smaller than those of three other dinucleotide models. The HOMOs and LUMOs of 5′-^{bt}UY-3′ show almost the same shape, area, and distribution as those of ^{bt}Ura itself (Figure S7), and the HOMO of 5′-G^{bt}U-3′ containing a protonated 5′-G is localized only on the ^{bt}Ura moiety (Figure S8). These results suggest that the much lower fluorescence of DNA containing the 5′-G^{bt}U-3′ sequence in basic solution results from the much wider area of overlap between the stacked bases and the accompanying delocalization of the HOMO and that deprotonation of the ^{bt}Ura and Gua bases is also an important contributor to the fluorescence. However, most of the fluorescent base analogues previously reported have a much lower intensity in ODNs than in the base or in the nucleoside itself, as a result of the sensitivity to its microenvironment, with the exception of tricyclic cytosine analogues, 1,3-diaza-2-oxo-phenothiazine (tC) and 1,3-diaza-2-oxo-phenoxazine (tC^{O}).[18] Therefore, d^{bt}U is still a promising fluorescent analogue that shows a low sensitivity to its microenvironment.

Conclusions

We have synthesized 11 fluorescent 5-(benzothiazol-2-yl)-2′-deoxyuridine derivatives and studied their photophysical properties. We found that 5-(5,6-dimethoxybenzothiazol-2-yl)-2′-deoxyuridine (d^{bt}U) has the highest quantum yield and fluorescence in an aqueous 100 mM NaOH solution, with a 113-nm Stokes shift, among the substituted benzothiazole derivatives of 2′-deoxyuridine. ODNs containing d^{bt}U were synthesized by using the phosphoramidite **6**, and their fluorescence properties were investigated. The fluorescence of the ODNs containing d^{bt}U has the same tendency as that of d^{bt}U itself, that is, weaker in neutral and stronger in basic solutions. These results reveal that the good fluorescence properties of d^{bt}U are maintained in the ODNs. The fluorescence intensity of the duplex ODN-d^{bt}U is slightly affected by a base at the site opposite in a complementary strand. From a sequence–fluorescence intensity and -quantum yield relationship study with ODNs containing 16 combinations of 5′- and 3′-neighboring sequences in aqueous 100 mM NaOH, only the 5′-G^{bt}U-3′ sequence has a much lower fluorescence intensity (7.9-fold lower on average), while the other sequences, including the 5′-^{bt}UG-3′ sequence, do not. Therefore, we calculated the ab initio HOMO and LUMO levels of stacked 5′-X^{bt}U-3′ and 5′-^{bt}UY-3′ (X, Y = A, G, C and T) dinucleotide models. The reason for the lower fluorescence of the ODN containing the 5′-G^{bt}U-3′ sequence in basic solution could be because the sequence has a wider area of overlap between the stacked Gua and ^{bt}Ura than that for the 5′-^{bt}UG-3′ sequence, and the HOMO delocalizes not only on ^{bt}Ura but also on Gua. Moreover, deprotonation of the ^{bt}U and G bases could also contribute to its fluorescence intensity (Figure S8). However, d^{bt}U is still a promising fluorescent analogue that shows low sensitivity to its microenvironment for detecting ^{fo}Ura in DNA. Compound d^{bt}U and its related compounds should lead to future applications in studies of the structure, dynamics, and interactions of DNA/RNA and in molecular diagnostics and biotechnology.

Experimental Section

General: ^{1}H, ^{13}C, and ^{31}P NMR spectra were obtained on JEOL ECX-400P and JEOL ECA-500 instruments and are reported in parts per million (δ) relative to the solvent signal for the ^{1}H NMR spectra and ^{13}C NMR spectra and 85% phosphoric acid (δ =0.0 ppm) as external standard for the ^{31}P NMR spectra. Coupling constants (J) are reported in Hertz [Hz]. LR- and HR-MS spectra were obtained on a JEOL JMS-T100LP, JEOL JMS-T100GCV or Thermo Scientific Exactive instrument. UV spectra were measured with Shimadzu UV Visible Spectrophotometer UV-2450. The pH was measured with a Beckman Coulter F360 pH meter. ODNs were prepared on an Applied Biosystems 3400 DNA Synthesizer. CD spectra were measured with a JASCO J-720 spectropolarimeter. Fluorescence spectra were measured with a JASCO FP-750 spectrofluorometer. HPLC was performed with Shimadzu LC-10AD-VP or LC-20AB (pump), Shimadzu SPD-M10A-VP or SPD-M20A (UV/Vis detector), Shimadzu CTO-10AS-VP or CTO-20A (column oven) instruments, CLASS-VP system, LabSolutions (system controller). Sep-pak Plus C18 Cartridge was purchased from Waters. YMC J'sphere ODS-M80 (150 × 4.6 mm) and SHISEIDO CAPCELL PAK C18 MG S-5 (250 × 4.6 mm) were used as reversed-phase C18 HPLC columns. Filtration of enzymes was performed by a Ultrafree®-Centrifugal Filter Unit (MILLIPORE). Snake venom phosphodiesterase (SVPD) was purchased from Funakoshi Co., Ltd. Nuclease P1 was purchased from Yamasa Co., Ltd. Calf intestine alkaline phosphatase was purchased from Takara Bio Inc. Incubation of enzymatic reactions was performed with EYELA MG-1200.

2-Amino-6-nitrobenzothiazole (2b): Bromine (0.56 mL, 11 mmol) was added dropwise to a suspension of NH_4SCN (1.7 g, 22 mmol) in AcOH (50 mL) at 10 °C, and the reaction mixture was stirred at the same temperature for 0.5 h. After filtration of the insoluble materials, the filtrate was added to a solution of 4-nitroaniline (1.4 g, 10 mmol) in AcOH (50 mL), and the reaction mixture was stirred at the same temperature for 19 h. After removal of the solvent in vacuo, the residue was diluted with AcOEt (100 mL). The organic layer was washed with saturated aqueous $NaHCO_3$

(50 mL × 3) and brine (50 mL), dried (Na_2SO_4), filtered, and concentrated. The residue was purified by column chromatography (SiO_2, MeOH in $CHCl_3$, 0–2%) to give **2b** (0.30 g, 1.5 mmol, 15%) as a yellow solid. ^{1}H NMR (500 MHz, [D_6]DMSO): δ = 8.68 (d, J = 2.3 Hz, 1 H, 7-H), 8.24 (s, 2 H, NH_2), 8.10 (dd, J = 8.6, 2.3 Hz, 1 H, 5-H), 7.41 (d, J = 8.6 Hz, 1 H, 4-H) ppm.

2-Amino-6-fluorobenzothiazole (2c): Compound **2c** (3.7 g, 21 mmol, 71%, as a yellow solid) was obtained from 4-fluoroaniline (2.8 mL, 30 mmol), NH_4SCN (3.4 g, 45 mmol), and bromine (1.8 mL, 36 mmol) as described for the synthesis of **2b**. ^{1}H NMR (400 MHz, $CDCl_3$): δ = 7.49 (dd, J = 9.1, 5.0 Hz, 1 H, 4-H), 7.32 (dd, J = 8.2, 2.7 Hz, 1 H, 7-H), 7.06 (dt, J = 9.1, 2.7 Hz, 1 H, 5-H), 5.18 (br. s, 2 H, NH_2) ppm.

2-Amino-6-chlorobenzothiazole (2d): Compound **2d** (1.5 g, 7.9 mmol, 79%, as a yellow solid) was obtained from 4-chloroaniline (1.3 g, 10 mmol), NH_4SCN (1.5 g, 20 mmol), and bromine (0.56 mL, 11 mmol) as described for the synthesis of **2b**. ^{1}H NMR (500 MHz, [D_6]DMSO): δ = 7.76 (d, J = 2.3 Hz, 1 H, 7-H), 7.59 (br. s, 2 H, NH_2), 7.29 (d, J = 8.6 Hz, 1 H, 4-H), 7.21 (dd, J = 8.6, 2.3 Hz, 1 H, 5-H) ppm.

2-Amino-6-bromobenzothiazole (2e): Compound **2e** (3.7 g, 21 mmol, 71%, as a yellow solid) was obtained from 4-bromoaniline (2.8 mL, 30 mmol), NH_4SCN (3.4 g, 45 mmol), and bromine (1.8 mL, 36 mmol) as described for the synthesis of **2b**, with the exception that hexane/AcOEt was used for crystallization. ^{1}H NMR (500 MHz, [D_6]DMSO): δ = 7.88 (d, J = 2.3 Hz, 1 H, 7-H), 7.60 (br. s, 2 H, NH_2), 7.32 (dd, J = 8.6, 2.3 Hz, 1 H, 5-H), 7.23 (d, J = 8.6 Hz, 1 H, 4-H) ppm.

2-Amino-6-iodobenzothiazole (2f): Compound **2f** (1.7 g, 6.1 mmol, 30%, as a yellow solid) was obtained from 4-iodoaniline (4.4 g, 20 mmol), NH_4SCN (2.7 g, 36 mmol), and bromine (1.2 mL, 24 mmol) as described for the synthesis of **2b**. ^{1}H NMR (500 MHz, [D_6]DMSO): δ = 8.00 (d, J = 1.7 Hz, 1 H, 7-H), 7.59 (br. s, 2 H, NH_2), 7.47 (dd, J = 8.6, 1.7 Hz, 1 H, 5-H), 7.12 (d, J = 8.6 Hz, 1 H, 4-H) ppm.

2-Amino-6-ethylbenzothiazole (2g): Compound **2g** (2.7 g, 15 mmol, 76%, as a yellow solid) was obtained from 4-ethylaniline (2.5 mL, 20 mmol), NH_4SCN (3.7 g, 48 mmol), and bromine (1.2 mL, 24 mmol) as described for the synthesis of **2b**. ^{1}H NMR (500 MHz, [D_6]DMSO): δ = 7.46 (s, 1 H, 7-H), 7.23 (br. s, 2 H, NH_2), 7.23 (d, J = 8.0 Hz, 1 H, 5-H), 7.03 (d, J = 8.0 Hz, 1 H, 4-H), 2.61 (q, J = 7.4 Hz, 2 H, CH_2CH_3), 1.18 (t, J = 7.4 Hz, 3 H, CH_2CH_3) ppm.

2-Amino-6-methoxybenzothiazole (2h): Compound **2h** (1.4 g, 7.5 mmol, 75%, as a purple solid) was obtained from 4-methoxyaniline (1.2 g, 10 mmol), NH_4SCN (1.8 g, 24 mmol), and bromine (0.61 mL, 12 mmol) as described for the synthesis of **2b**. ^{1}H NMR (400 MHz, [D_6]DMSO): δ = 7.28 (d, J = 2.3 Hz, 1 H, 7-H), 7.22 (d, J = 8.6 Hz, 1 H, 4-H), 7.21 (br. s, 2 H, NH_2), 6.80 (dd, J = 8.6, 2.3 Hz, 1 H, 5-H), 3.72 (s, 3 H, CH_3O) ppm.

2-Amino-5,6-dimethoxybenzothiazole (2i): Compound **2i** (4.5 g, 24 mmol, 78%, as a purple solid) was obtained from 3,4-dimethoxyaniline (4.6 g, 30 mmol), NH_4SCN (4.1 g, 54 mmol), and bromine (1.8 mL, 36 mmol) as described for the synthesis of **2b**. ^{1}H NMR (500 MHz, $CDCl_3$): δ = 7.11, 7.01 (each s, each 1 H, 4-H and 7-H), 5.22 (br. s, 2 H, NH_2), 3.89 (s, 6 H, $CH_3O \times 2$) ppm.

2-Amino-4,6-dimethoxybenzothiazole (2j): Compound **2j** (1.2 g, 5.5 mmol, 28%, as a red solid) was obtained from 2,4-dimethoxyaniline (3.1 g, 20 mmol), NH_4SCN (2.7 g, 36 mmol), and bromine (1.2 mL, 24 mmol) as described for the synthesis of **2b**. ^{1}H NMR (400 MHz, $CDCl_3$): δ = 6.72, 6.45 (each d, J = 1.8 Hz, each 1 H, 5-H and 7-H), 5.15 (br. s, 2 H, NH_2), 3.93, 3.82 (each s, each 3 H, CH_3O) ppm.

2-Amino-5,6,7-trimethoxybenzothiazole (2k): Compound **2k** (2.2 g, 9.3 mmol, 47%, as a pale yellow solid) was obtained from 3,4,5-trimethoxyaniline (3.7 g, 20 mmol), NH_4SCN (2.3 g, 30 mmol), and bromine (1.1 mL, 22 mmol) as described for the synthesis of **2b**. ^{1}H NMR (400 MHz, $CDCl_3$): δ = 6.90 (s, 1 H, 4-H), 5.08 (br. s, 2 H, NH_2), 4.02, 3.89, 3.87 (each s, each 3 H, CH_3O) ppm.

6-Acetylamino-2-aminobenzothiazole (2l): A solution of Ac_2O (1.9 mL, 20 mmol) in THF (4 mL) was added dropwise to a solution of *p*-phenylenediamine (2.2 g, 20 mmol), and the reaction mixture was stirred at room temperature for 24 h. The pale pink insoluble compounds were filtered, washed with cold THF, and dissolved in hot MeOH. After cooling of the solution, the precipitate was filtered off, and the filtrate was concentrated to give a mixture of **1l** (1.9 g, 13 mmol, 63%) and the diacetylated product (7%) as a white solid. Bromine (0.77 mL, 15 mmol) was added dropwise to a suspension of NH_4SCN (2.3 g, 30 mmol) in AcOH (20 mL) at 10 °C, and the reaction mixture was stirred at the same temperature for 0.5 h. After filtration of the insoluble materials, the filtrate was added to a solution of **1l** (1.9 g, 13 mmol) in AcOH (20 mL), and the reaction mixture was stirred at the same temperature for 18 h. The brown insoluble compounds were removed by filtration and washed with cold THF to give **2l** (2.3 g, 11 mmol, 88%) as a pale pink solid. ^{1}H NMR (500 MHz, [D_6]DMSO): δ = 10.12 (s, 1 H, NHAc), 9.32 (br. s, 2 H, NH_2), 8.25 (d, J = 1.7 Hz, 1 H, 7-H), 7.45 (dd, J = 8.6, 1.7 Hz, 1 H, 5-H), 7.39 (d, J = 8.6 Hz, 1 H, 4-H), 2.04 (s, 3 H, CH_3CO) ppm.

Bis(anilin-2-yl)disulfide (3a): A suspension of **2a** (1.5 g, 10 mmol) and ethylene glycol (2.2 mL, 40 mmol) in aqueous KOH (3.0 M, 100 mL) was stirred at 140 °C for 24 h. After cooling of the mixture, it was neutralized with concentrated HCl on an ice bath, and the precipitate was filtered off and washed with AcOEt. The filtrate was partitioned between AcOEt (200 mL) and H_2O (200 mL). The water layer was extracted with AcOEt (80 mL × 2), and the combined organic layer was washed with brine (200 mL), dried (Na_2SO_4), filtered, and concentrated. The residue was crystallized from hexane/AcOEt to give **3a** (0.75 g, 3.0 mmol, 61%) as a yellow solid. ^{1}H NMR (400 MHz, [D_6]DMSO): δ = 7.07 (dt, J = 8.3, 8.3, 1.8 Hz, 2 H, 4-H), 6.98 (dd, J = 7.7, 1.8 Hz, 2 H, 6-H), 6.71 (dd, J = 8.3, 0.9 Hz, 2 H, 3-H), 6.41 (ddd, J = 8.3, 7.7, 0.9 Hz, 2 H, 5-H), 5.45 (br. s, 4 H, NH_2) ppm.

2-Amino-5-nitrothiophenol (3′b): A suspension of **2b** (3.9 g, 20 mmol) and ethylene glycol (4.5 mL, 80 mmol) in aqueous KOH (3.0 M, 200 mL) was stirred at 140 °C for 24 h. After cooling of the mixture, it was neutralized with concentrated HCl on an ice bath and washed with $CHCl_3$ (200 mL × 3). The combined organic layer was washed with brine (200 mL), dried (Na_2SO_4), filtered, and concentrated. The residue was crystallized from hexane/AcOEt to give **3′b** (2.1 g, 13 mmol, 63%) as a yellow solid. ^{1}H NMR (400 MHz, [D_6]DMSO): δ = 8.25 (d, J = 2.7 Hz, 1 H, 6-H), 7.88 (dd, J = 8.6, 2.7 Hz, 1 H, 4-H), 6.93 (d, J = 8.6 Hz, 1 H, 3-H) ppm.

Bis(5-fluoroanilin-2-yl)disulfide (3c): Compound **3c** (1.3 g, 4.6 mmol, 92%, as a green solid) was obtained from **2c** (1.7 g, 10 mmol) and ethylene glycol (2.2 mL, 40 mmol) in aqueous KOH (3.0 M, 50 mL) as described for the synthesis of **3a**. ^{1}H NMR (500 MHz, [D_6]DMSO): δ = 6.98 (dt, J = 8.6, 2.9 Hz, 2 H, 4-H), 6.83 (dd, J = 8.6, 2.9 Hz, 2 H, 6-H), 6.73 (dd, J = 8.6, 5.2 Hz, 2 H, 3-H), 5.35 (br. s, 4 H, NH_2) ppm.

Bis(5-chloroanilin-2-yl)disulfide (3d): Compound **3d** (1.9 g, 6.0 mmol, 79%, as a green solid) was obtained from **2d** (2.8 g,

15 mmol) and ethylene glycol (3.6 mL, 60 mmol) in aqueous KOH (3.0 M, 75 mL) as described for the synthesis of **3a**. ^{1}H NMR (500 MHz, [D$_6$]DMSO): δ = 7.13 (d, J = 6.9 Hz, 2 H, 5-H), 6.88 (s, 2 H, 3-H), 6.75 (d, J = 6.9 Hz, 2 H, 6-H), 5.71 (s, 4 H, NH$_2$) ppm.

Bis(5-bromoanilin-2-yl)disulfide (3e): Compound **3e** (0.69 g, 1.7 mmol, 68%, as a yellow solid) was obtained from **2e** (1.2 g, 5.0 mmol) and ethylene glycol (1.1 mL, 20 mmol) in aqueous KOH (3.0 M, 50 mL) as described for the synthesis of **3a**, with the exception that the purification step was performed with column chromatography (SiO$_2$, AcOEt in hexane, 0–80%). ^{1}H NMR (500 MHz, [D$_6$]DMSO): δ = 7.30 (d, J = 2.3 Hz, 2 H, 6-H), 7.03 (dd, J = 8.6, 2.3 Hz, 2 H, 4-H), 6.63 (d, J = 8.6 Hz, 2 H, 3-H), 5.30 (br. s, 4 H, NH$_2$) ppm.

Bis(5-iodoanilin-2-yl)disulfide (3f): Compound **3f** (0.37 g, 0.73 mmol, 49%, as a yellow solid) was obtained from **2f** (0.83 g, 3.0 mmol) and ethylene glycol (0.67 mL, 12 mmol) in aqueous KOH (3.0 M, 30 mL) as described for the synthesis of **3e**. ^{1}H NMR (500 MHz, [D$_6$]DMSO): δ = 7.35 (dd, J = 8.6, 2.3 Hz, 2 H, 4-H), 7.10 (d, J = 2.3 Hz, 2 H, 6-H), 6.59 (d, J = 8.6 Hz, 2 H, 3-H), 5.75 (br. s, 4 H, NH$_2$) ppm. ^{13}C NMR (125 MHz, [D$_6$]DMSO): δ = 149.5, 142.8, 139.3, 118.3, 117.2, 75.2 ppm. EIMS-LR: m/z = 500 [M]$^+$. EIMS-HR: calcd. for C$_{12}$H$_{10}$I$_2$N$_2$S$_2$ 499.8375; found 499.8371.

Bis(5-ethylanilin-2-yl)disulfide (3g): Compound **3g** (1.6 g, 5.2 mmol, 68%, as a green solid) was obtained from **2g** (2.7 g, 15 mmol) and ethylene glycol (3.4 mL, 60 mmol) in aqueous KOH (10 M, 50 mL) as described for the synthesis of **3a**. ^{1}H NMR (400 MHz, [D$_6$]-DMSO): δ = 6.95 (dd, J = 8.2, 1.8 Hz, 2 H, 4-H), 6.78 (d, J = 1.8 Hz, 2 H, 6-H), 6.67 (d, J = 8.2 Hz, 2 H, 3-H), 5.26 (br. s, 4 H, NH$_2$), 2.35 (q, J = 7.7 Hz, 4 H, CH$_2$CH$_3$), 1.02 (t, J = 7.7 Hz, 6 H, CH$_2$CH$_3$) ppm.

Bis(5-methoxyanilin-2-yl)disulfide (3h): Compound **3h** (1.2 g, 3.9 mmol, 74%, as a green solid) was obtained from **2h** (1.9 g, 11 mmol) and ethylene glycol (2.2 mL, 40 mmol) in aqueous KOH (3.0 M, 50 mL) as described for the synthesis of **3a**. ^{1}H NMR (400 MHz, [D$_6$]DMSO): δ = 6.77 (dd, J = 8.5, 3.2 Hz, 2 H, 5-H), 6.69 (d, J = 8.5 Hz, 2 H, 6-H), 6.58 (d, J = 3.2 Hz, 2 H, 3-H), 5.04 (s, 4 H, NH$_2$), 3.51 (s, 6 H, OCH$_3$) ppm.

Bis(4,5-dimethoxyanilin-2-yl)disulfide (3i): Compound **3i** (3.5 g, 9.6 mmol, 82%, as a yellow solid) was obtained from **2i** (4.9 g, 24 mmol) and ethylene glycol (5.6 mL, 100 mmol) in aqueous KOH (3.0 M, 80 mL) as described for the synthesis of **3e**. ^{1}H NMR (400 MHz, [D$_6$]DMSO): δ = 6.44, 6.41 (each s, each 2 H, 3-H and 6-H), 5.15 (br. s, 4 H, NH$_2$), 3.70, 3.47 (each s, each 6 H, OCH$_3$ × 2) ppm.

Bis(3,5-Dimethoxyanilin-2-yl)disulfide (3j): Compound **3j** (0.41 g, 1.1 mmol, 50%, as a green solid) was obtained from **2j** (1.2 g, 5.5 mmol) and ethylene glycol (1.2 mL, 22 mmol) in aqueous KOH (10 M, 55 mL) as described for the synthesis of **3e**. ^{1}H NMR (400 MHz, [D$_6$]DMSO): δ = 6.53, 6.27 (each s, each 2 H, 4-H and 6-H), 4.58 (br. s, 4 H, NH$_2$), 3.76, 3.54 (each s, each 6 H, OCH$_3$ × 2) ppm. ^{13}C NMR (125 MHz, [D$_6$]DMSO): δ = 150.0, 147.5, 133.4, 116.6, 108.7, 101.6, 55.8, 55.2 ppm. EIMS-LR: m/z = 368 [M]$^+$. EIMS-HR: calcd. for C$_{16}$H$_{20}$N$_2$O$_4$S$_2$ 368.0865; found 368.0871.

Bis(4,5,6-trimethoxyanilin-2-yl)disulfide (3k): Compound **3k** (820 mg, 1.9 mmol, 77%, as a yellow foam) was obtained from **2k** (1.2 g, 5.0 mmol) and ethylene glycol (1.1 mL, 20 mmol) in aqueous KOH (6.0 M, 50 mL) as described for the synthesis of **3e**. ^{1}H NMR (500 MHz, [D$_6$]DMSO): δ = 6.14 (s, each 2 H, 3-H), 5.24 (br. s, 4 H, NH$_2$), 3.69 (s, 6 H, OCH$_3$ × 2) 3.55 (s, 12 H, OCH$_3$ × 4) ppm. ^{13}C NMR (125 MHz, [D$_6$]DMSO): δ = 155.9, 155.1, 148.2, 132.7, 102.6, 93.5, 60.9, 60.5, 55.4 ppm. EIMS-LR: m/z = 428 [M]$^+$. EIMS-HR: calcd. for C$_{18}$H$_{24}$N$_2$O$_6$S$_2$ 428.1076; found 428.1079.

5-Benzothiazol-2-yl-2′-deoxyuridine (4a): A solution of **3a** (75 mg, 0.30 mmol) and (±)-DTT (93 mg, 0.60 mmol) in DMF (3 mL) was stirred at room temperature for 0.5 h. d^{fo}U (77 mg, 0.30 mmol) was added to the solution, and the reaction mixture was stirred at room temperature for 1 h. Sc(OTf)$_3$ (15 mg, 0.030 mmol) and aqueous H$_2$O$_2$ (35%, 60 μL, 0.90 mmol) were added to the mixture, which was further stirred under O$_2$ at room temperature for 1 h. After the removal of the solvent in vacuo, the residue was washed with AcOEt, and the insoluble material was filtered to give **4a** (89 mg, 0.25 mmol, 82%) as a pale pink solid. The sample for elemental analysis and fluorescence experiments was obtained by crystallization from aq. EtOH as a white crystal (255 °C colored). UV: λ_{max} (ε, M^{-1} cm^{-1}) = 335 (14700) (aq. 100 mM HCl), 324 (14800) (10 mM phosphate buffer, pH 7.0), 325 (17600) (aq. 100 mM NaOH) nm. ^{1}H NMR (500 MHz, [D$_6$]DMSO): δ = 12.02 (s, 1 H, NH), 9.11 (s, 1 H, 6-H), 8.07, 7.95 (each d, J = 8.0, 8.0 Hz, each 1 H, 4′′-H and 7′′-H), 7.94 (d, J = 8.6 Hz, 1 H), 7.53 (dd, J = 8.6, 2.3 Hz, 1 H, 5′′-H), 6.20 (t, J = 5.9 Hz, 1 H, 1′-H), 5.33 (d, J = 4.5 Hz, 1 H, OH-3′), 5.12 (t, J = 3.6 Hz, 1 H, OH-5′), 4.30 (m, 1 H, 3′-H), 3.90 (d, 1 H, 4′-H), 3.68 (m, 2 H, 5′-H), 2.27 (m, 2 H, 2′-H) ppm. ^{13}C NMR (100 MHz, [D$_6$]DMSO): δ = 161.6, 159.6, 151.5, 149.4, 141.1, 134.8, 126.2, 124.4, 121.9, 106.9, 87.9, 85.8, 70.3, 61.1, 40.4 ppm. ESI-MS (LR): m/z = 360 [M – H]$^-$. C$_{16}$H$_{15}$N$_3$O$_5$S·3/10H$_2$O: calcd. C 52.40, H 4.29, N 11.46, S 8.74; found C 52.54, H 4.33, N 11.23, S 8.76.

5-(6-Fluorobenzothiazol-2-yl)-2′-deoxyuridine (4c): Compound **4c** (78 mg, 0.21 mmol, 69%, as a white solid) was obtained from d^{fo}U (77 mg, 0.30 mmol), **3c** (85 mg, 0.30 mmol), (±)-DTT (230 mg, 1.5 mmol), Sc(OTf)$_3$ (15 mg, 0.030 mmol), and aqueous H$_2$O$_2$ (35%, 96 μL, 1.5 mmol) as described for the synthesis of **4a**, with the exception that the purification step involved crystallization from aq. EtOH following column chromatography (SiO$_2$, MeOH in CHCl$_3$, 0–4%, 255 °C colored). UV: λ_{max} (ε, M^{-1} cm^{-1}) = 329 (17400) (aq. 100 mM HCl), 326 (17700) (10 mM phosphate buffer, pH 7.0), 326 (19700) (aq. 100 mM NaOH) nm. ^{1}H NMR (500 MHz, [D$_6$]DMSO): δ = 12.04 (br. s, 1 H, NH), 9.11 (s, 1 H, 6-H), 7.95 (m, 2 H, Ar-H), 7.35 (m, 1 H, Ar-H), 6.19 (t, J = 6.3 Hz, 1 H, 1′-H), 5.32 (d, J = 4.0 Hz, 1 H, OH-3′), 5.10 (t, J = 4.6 Hz, 1 H, OH-5′), 4.29 (m, 1 H, 3′-H), 3.90 (d, J = 3.4 Hz, 1 H, 4′-H), 3.64 (m, 2 H, 5′-H), 2.27 (m, 2 H, 2′-H) ppm. ^{13}C NMR (125 MHz, [D$_6$]-DMSO): δ = 161.7, 159.9, 158.3, 149.4, 148.4, 141.2, 136.1, 136.1, 106.8, 88.0, 85.9, 70.3, 61.1, 40.5 ppm. ESI-MS (LR): m/z = 378 [M – H]$^-$. C$_{16}$H$_{14}$FN$_3$O$_5$S (379.36): calcd. C 50.66, H 3.72, N 11.08, S 8.45; found C 50.28, H 3.74, N 10.89, S 8.67.

5-(6-Chlorobenzothiazol-2-yl)-2′-deoxyuridine (4d): Compound **4d** (73 mg, 0.18 mmol, 92%, as a yellow solid) was obtained from d^{fo}U (51 mg, 0.20 mmol), **3d** (64 mg, 0.20 mmol), (±)-DTT (31 mg, 0.20 mmol), Sc(OTf)$_3$ (10 mg, 0.020 mmol), and aqueous H$_2$O$_2$ (35%, 13 μL, 0.20 mmol) as described for the synthesis of **4c**. The sample for elemental analysis and fluorescence experiments was obtained by crystallization from aq. EtOH as a white crystal (260 °C colored). UV: λ_{max} (ε, M^{-1} cm^{-1}) = 331 (6100) (aq. 100 mM HCl), 330 (6500) (10 mM phosphate buffer, pH 7.0), 330 (19000) (aq. 100 mM NaOH) nm. ^{1}H NMR (400 MHz, [D$_6$]DMSO): δ = 12.07 (br. s, 1 H, NH), 9.15 (s, 1 H, 6-H), 8.22 (d, J = 2.3 Hz, 1 H, 7′′-H), 7.93 (d, J = 8.6 Hz, 1 H, 4′′-H), 7.51 (dd, J = 8.6, 2.3 Hz, 1 H, 5′′-H), 6.18 (t, J = 6.3 Hz, 1 H, 1′-H), 5.31 (d, J = 4.6 Hz, 1 H, OH-3′), 5.10 (t, J = 5.2 Hz, 1 H, OH-5′), 4.29 (m, 1 H, 3′-H), 3.90 (m, 1 H, 4′-H), 3.65 (m, 2 H, 5′-H), 2.26 (m, 2 H, 2′-H) ppm. ^{13}C NMR

(125 MHz, [D$_6$]DMSO): δ = 161.6, 160.7, 150.3, 149.3, 141.5, 136.4, 128.7, 126.6, 123.1, 121.6, 106.6, 88.0, 85.9, 70.2, 61.0, 40.5 ppm. ESI-MS (LR): *m/z* = 396 [M + H]$^+$. $C_{16}H_{14}ClN_3O_5S$ (395.82): calcd. C 48.55, H 3.57, Cl 8.96, N 10.62, S 8.16; found C 48.15, H 3.76, Cl 8.67, N 10.39, S 7.77.

5-(6-Bromobenzothiazol-2-yl)-2′-deoxyuridine (4e): Compound **4e** (130 mg, 0.29 mmol, 97%, as a yellow solid) was obtained from d^{fo}U (77 mg, 0.30 mmol), **3e** (120 mg, 0.30 mmol), (±)-DTT (93 mg, 0.60 mmol), Sc(OTf)$_3$ (15 mg, 0.030 mmol), and aqueous H_2O_2 (35%, 58 μL, 0.90 mmol) as described for the synthesis of **4a**. The sample for fluorescence experiments was obtained by crystallization from aq. EtOH as a yellow crystal (255 °C colored). UV: λ_{max} (ε, M^{-1}cm^{-1}) = 333 (16300) (aq. 100 mM HCl), 330 (16500) (10 mM phosphate buffer, pH 7.0), 331 (20300) (aq. 100 mM NaOH) nm. ^{1}H NMR (400 MHz, [D$_6$]DMSO): δ = 12.06 (br. s, 1 H, NH), 9.16 (s, 1 H, 6-H), 8.36 (d, *J* = 1.8 Hz, 1 H, 7′′-H), 7.87 (d, *J* = 8.6 Hz, 1 H, 4′′-H), 7.63 (dd, *J* = 8.6, 1.8 Hz, 1 H, 5′′-H), 6.18 (t, *J* = 6.3 Hz, 1 H, 1′-H), 5.32 (d, *J* = 4.1 Hz, 1 H, OH-3′), 5.11 (t, *J* = 4.5 Hz, 1 H, OH-5′), 4.29 (m, 1 H, 3′-H), 3.90 (m, 1 H, 4′-H), 3.65 (m, 2 H, 5′-H), 2.26 (m, 2 H, 2′-H) ppm. ^{13}C NMR (100 MHz, [D$_6$]DMSO): δ = 161.6, 160.7, 150.6, 149.3, 141.6, 136.9, 129.3, 124.5, 123.5, 116.8, 106.6, 88.0, 85.9, 70.2, 61.0, 40.5 ppm. ESI-MS (LR): *m/z* = 438, 440 [M – H]$^-$. ESI-MS (HR): calcd. for $C_{16}H_{13}BrN_3O_5S$ 437.9768; found 437.9781.

5-(6-Iodobenzothiazol-2-yl)-2′-deoxyuridine (4f): Compound **4f** (96 mg, 0.20 mmol, 66%, as a white solid) was obtained from d^{fo}U (77 mg, 0.30 mmol), **3f** (150 mg, 0.30 mmol), (±)-DTT (230 mg, 1.5 mmol), Sc(OTf)$_3$ (15 mg, 0.030 mmol), and aqueous H_2O_2 (35%, 96 μL, 1.5 mmol) as described for the synthesis of **4c**. The sample for elemental analysis and fluorescence experiments was obtained by crystallization from aq. EtOH as a white crystal (262 °C colored). UV: λ_{max} (ε, M^{-1}cm^{-1}) = 332 (10100) (aq. 100 mM HCl), 332 (10000) (10 mM phosphate buffer, pH 7.0), 332 (24000) (aq. 100 mM NaOH) nm. ^{1}H NMR (500 MHz, [D$_6$]DMSO): δ = 12.05 (br. s, 1 H, NH), 9.15 (s, 1 H, 6-H), 8.49 (s, 1 H, 7′′-H), 7.77, 7.73 (each d, *J* = 8.6 Hz, each 1 H, 4′′-H and 5′′-H), 6.18 (t, 1 H, 1′-H, *J* = 6.3 Hz), 5.32 (d, *J* = 4.0 Hz, 1 H, OH-3′), 5.10 (t, *J* = 4.0 Hz, 1 H, OH-5′), 4.29 (m, 1 H, 3′-H), 3.90 (m, 1 H, 4′-H), 3.64 (m, 2 H, 5′-H), 2.26 (m, 2 H, 2′-H) ppm. ^{13}C NMR (100 MHz, [D$_6$]DMSO): δ = 161.6, 160.4, 151.0, 149.3, 141.6, 137.3, 134.8, 130.2, 123.7, 106.6, 89.1, 88.0, 85.9, 70.2, 61.0, 40.5 ppm. ESI-MS (LR): *m/z* = 486 [M – H]$^-$. $C_{16}H_{14}IN_3O_5S$ (487.27): calcd. C 39.44, H 2.90, N 8.62, S 6.58; found C 39.51, H 2.90, N 8.56, S 6.58.

5-(6-Ethylbenzothiazol-2-yl)-2′-deoxyuridine (4g): Compound **4g** (69 mg, 0.18 mmol, 59%, as a yellow solid) was obtained from d^{fo}U (77 mg, 0.30 mmol), **3g** (91 mg, 0.30 mmol), (±)-DTT (230 mg, 1.5 mmol), Sc(OTf)$_3$ (15 mg, 0.030 mmol), and aqueous H_2O_2 (35%, 96 μL, 1.5 mmol) as described for the synthesis of **4c**. The sample for elemental analysis and fluorescence experiments was obtained by crystallization from aq. EtOH as a white crystal (250 °C colored). UV: λ_{max} (ε, M^{-1}cm^{-1}) = 345 (9100) (aq. 100 mM HCl), 331 (8300) (10 mM phosphate buffer, pH 7.0), 332 (15600) (aq. 100 mM NaOH) nm. ^{1}H NMR (500 MHz, [D$_6$]DMSO): δ = 12.00 (br. s, 1 H, NH), 9.06 (s, 1 H, 6-H), 7.88 (s, 1 H, 7′′-H), 7.84 (d, *J* = 8.6 Hz, 1 H, 4′′-H), 7.34 (d, *J* = 8.6 Hz, 1 H, 5′′-H), 6.19 (t, *J* = 6.3 Hz, 1 H, 1′-H), 5.32 (d, *J* = 4.0 Hz, 1 H, OH-3′), 5.07 (t, *J* = 4.6 Hz, 1 H, OH-5′), 4.29 (dd, *J* = 4.0, 3.4 Hz, 1 H, 3′-H), 3.89 (d, *J* = 3.4 Hz, 1 H, 4′-H), 3.68 (m, 2 H, 5′-H), 2.73 (q, *J* = 7.4 Hz, 2 H, CH_2CH_3), 2.25 (m, 2 H, 2′-H), 1.24 (t, *J* = 7.4 Hz, 3 H, CH_2CH_3) ppm. ^{13}C NMR (125 MHz, [D$_6$]DMSO): δ = 161.5, 158.5, 149.9, 149.4, 140.8, 140.4, 135.0, 126.6, 121.6, 120.3, 107.1, 87.9, 85.7, 70.3, 61.1, 40.4, 28.2, 15.9 ppm. ESI-MS (LR): *m/z* = 412 [M + Na]$^+$. $C_{18}H_{19}N_3O_5S\cdot1/5H_2O$: calcd. C 55.01, H 4.98, N 10.69, S 8.16; found C 55.00, H 4.93, N 10.49, S 8.03.

5-(6-Methoxybenzothiazol-2-yl)-2′-deoxyuridine (4h): Compound **4h** (64 mg, 0.16 mmol, 82%, as a yellow solid) was obtained from d^{fo}U (51 mg, 0.20 mmol), **3h** (62 mg, 0.20 mmol), (±)-DTT (31 mg, 0.20 mmol), Sc(OTf)$_3$ (10 mg, 0.020 mmol), and aqueous H_2O_2 (35%, 13 μL, 0.20 mmol) as described for the synthesis of **4c**. The sample for elemental analysis and fluorescence experiments was obtained by crystallization from aq. EtOH, as a yellow crystal (228 °C colored). UV: λ_{max} (ε, M^{-1}cm^{-1}) = 351 (14300) (aq. 100 mM HCl), 336 (14600) (10 mM phosphate buffer, pH 7.0), 335 (17600) (aq. 100 mM NaOH) nm. ^{1}H NMR (500 MHz, [D$_6$]DMSO): δ = 11.99 (s, 1 H, NH), 9.01 (s, 1 H, 6-H), 7.83 (d, *J* = 9.2 Hz, 1 H, 4′′-H), 7.63 (d, *J* = 2.3 Hz, 1 H, 7′′-H), 7.08 (dd, *J* = 9.2, 2.3 Hz, 1 H, 5′′-H), 6.19 (t, *J* = 6.3 Hz, 1 H, 1′-H), 5.31 (d, *J* = 4.6 Hz, 1 H, OH-3′), 5.07 (t, *J* = 4.6 Hz, 1 H, OH-5′), 4.29 (m, 1 H, 3′-H), 3.88 (m, 1 H, 4′-H), 3.82 (s, 3 H, CH_3O), 3.63 (m, 2 H, 5′-H), 2.25 (m, 2 H, 2′-H) ppm. ^{13}C NMR (125 MHz, [D$_6$]DMSO): δ = 161.5, 156.9, 156.8, 149.4, 146.0, 140.3, 136.3, 122.5, 115.6, 107.2, 104.3, 87.9, 85.7, 70.3, 61.1, 55.7, 40.4 ppm. ESI-MS (LR): *m/z* = 414 [M + Na]$^+$. $C_{17}H_{17}N_3O_6S\cdot2/5H_2O$: calcd. C 51.22, H 4.53, N 10.54, S 8.04; found C 51.18, H 4.37, N 10.26, S 7.80.

5-(5,6-Dimethoxybenzothiazol-2-yl)-2′-deoxyuridine (4i): Compound **4i** (95 mg, 0.23 mmol, 75%, as a yellow-green solid) was obtained from d^{fo}U (77 mg, 0.30 mmol), **3i** (110 mg, 0.30 mmol), (±)-DTT (46 mg, 0.30 mmol), Sc(OTf)$_3$ (15 mg, 0.030 mmol), and aqueous H_2O_2 (35%, 19 μL, 0.30 mmol) as described for the synthesis of **4c**. The sample for elemental analysis and fluorescence experiments was obtained by crystallization from aq. EtOH as a yellow–green crystal (236 °C colored). UV: λ_{max} (ε, M^{-1}cm^{-1}) = 368 (15900) (aq. 100 mM HCl), 351 (16600) (10 mM phosphate buffer, pH 7.0), 345 (20000) (aq. 100 mM NaOH) nm. ^{1}H NMR (500 MHz, [D$_6$]DMSO): δ = 11.95 (s, 1 H, NH), 8.98 (s, 1 H, 6-H), 7.60, 7.45 (each s, each 1 H, 4′′-H and 7′′-H), 6.19 (t, *J* = 6.3 Hz, 1 H, 1′-H), 5.30 (d, *J* = 4.6 Hz, 1 H, OH-3′), 5.07 (t, *J* = 4.6 Hz, 1 H, OH-5′), 4.28 (m, 1 H, 3′-H), 3.87 (d, *J* = 2.8 Hz, 1 H, 4′-H), 3.83, 3.81 (each s, each 3 H, $CH_3O\times2$), 3.63 (m, 2 H, 5′-H), 2.23 (m, 2 H, 2′-H) ppm. ^{13}C NMR (125 MHz, [D$_6$]DMSO): δ = 161.6, 157.2, 149.6, 149.3, 148.0, 146.1, 140.0, 127.1, 107.7, 104.1, 103.3, 88.0, 85.7, 70.5, 61.4, 56.1, 55.9, 39.9 ppm. ESI-MS (LR): *m/z* = 420 [M – H]$^-$. $C_{18}H_{19}N_3O_7S\cdot1/2H_2O$: calcd. C 50.23, H 4.68, N 9.76, S 7.45; found C 50.16, H 4.68, N 9.52, S 7.26.

5-(4,6-Dimethoxybenzothiazol-2-yl)-2′-deoxyuridine (4j): Compound **4j** (85 mg, 0.20 mmol, 67%, as a pale pink solid) was obtained from d^{fo}U (77 mg, 0.30 mmol), **3j** (110 mg, 0.30 mmol), (±)-DTT (230 mg, 1.5 mmol), Sc(OTf)$_3$ (15 mg, 0.030 mmol), and aqueous H_2O_2 (35%, 140 μL, 2.3 mmol) as described for the synthesis of **4c**. The sample for elemental analysis and fluorescence experiments was obtained by crystallization from aq. EtOH as a yellow crystal (218 °C colored). UV: λ_{max} (ε, M^{-1}cm^{-1}) = 345 (12900) (aq. 100 mM HCl), 341 (12000) (10 mM phosphate buffer, pH7.0),339(15500)(aq.100 mMNaOH)nm.^{1}HNMR(500 MHz,[D$_6$]-DMSO): δ = 11.98 (br. s, 1 H, NH), 8.79 (s, 1 H, 6-H), 7.19, 6.61 (each d, *J* = 2.3 Hz, each 1 H, 5′′-H and 7′′-H), 6.16 (t, *J* = 6.9 Hz, 1 H, 1′-H), 5.32 (d, *J* = 4.6 Hz, 1 H, OH-3′), 4.97 (t, *J* = 5.2 Hz, 1 H, OH-5′), 4.26 (m, 1 H, 3′-H), 3.94 (s, 3 H,CH_3O), 3.89 (dd, *J* = 7.4, 4.0 Hz, 1 H, 4′-H), 3.81 (s, 3 H, CH_3O), 3.59 (t, *J* = 4.6 Hz, 2 H, 5′-H), 2.25 (m, 2 H, 2′-H) ppm. ^{13}C NMR (100 MHz, [D$_6$]-DMSO): δ = 161.7, 158.1, 154.9, 153.0, 149.5, 139.7, 137.5, 136.7, 107.4, 98.6, 95.7, 88.1, 86.0, 70.6, 61.4, 56.3, 55.8, 40.2 ppm. ESI-MS (LR): *m/z* = 420 [M – H]$^-$. $C_{18}H_{19}N_3O_7S\cdot1/2H_2O$: calcd. C 50.23, H 4.68, N 9.76, S 7.45; found C 50.41, H 4.68, N 9.61, S 7.48.

5-(5,6,7-Trimethoxybenzothiazol-2-yl)-2′-deoxyuridine (4k): Compound **4k** (130 mg, 0.29 mmol, 98%, as a yellow solid) was obtained from $d^{fo}U$ (77 mg, 0.30 mmol), **3k** (100 mg, 0.24 mmol), (±)-DTT (230 mg, 1.5 mmol), $Sc(OTf)_3$ (15 mg, 0.030 mmol), and aqueous H_2O_2 (35%, 190 μL, 3.0 mmol) as described for the synthesis of **4c**. The sample for elemental analysis and fluorescence experiments was obtained by crystallization from aq. EtOH as a yellow crystal (260 °C colored). UV: λ_{max} (ε, $M^{-1}cm^{-1}$) = 347 (15800) (aq. 100 mM HCl), 343 (16100) (10 mM phosphate buffer, pH 7.0), 341 (19300) (aq. 100 mM NaOH) nm. ^{1}H NMR (500 MHz, [D$_6$]DMSO): δ = 12.02 (s, 1 H, NH), 9.05 (s, 1 H, 6-H), 7.32 (s, 1 H, 4′′-H), 6.18 (t, J = 6.3 Hz, 1 H, 1′-H), 5.32 (d, J = 4.0 Hz, 1 H, OH-3′), 5.08 (t, J = 4.6 Hz, 1 H, OH-5′), 4.29 (m, 1 H, 3′-H), 3.90 (s, 3 H, CH_3O), 3.90–3.88 (m, total 4 H, 4′-H and CH_3O), 3.79 (s, 3 H, CH_3O), 3.64 (m, J = 4.6 Hz, 2 H, 5′-H), 2.25 (m, 2 H, 2′-H) ppm. ^{13}C NMR (100 MHz, [D$_6$]DMSO): δ = 161.5, 159.0, 153.6, 149.4, 148.1, 146.2, 140.6, 138.6, 119.7, 107.0, 100.2, 87.9, 85.7, 70.3, 61.1, 61.1, 60.4, 56.2, 40.5 ppm. ESI-MS (LR): m/z = 450 [M – H]$^-$. $C_{19}H_{21}N_3O_8S$ (451.45): calcd. C 50.55, H 4.69, N 9.31, S 7.10; found C 50.61, H 4.68, N 9.17, S 6.96.

5-(6-Aminobenzothiazol-2-yl)-2′-deoxyuridine (4l): A suspension of **2l** (1.0 g, 5.0 mmol) and ethylene glycol (1.1 mL, 20 mmol) in aqueous KOH (3.0 M, 75 mL) was stirred at 140 °C for 24 h. After cooling of the mixture, it was neutralized with concentrated HCl on an ice bath, and the precipitate was filtered and washed with $CHCl_3$/MeOH [1:1 (v/v)]. The organic solution was concentrated, and the residue was roughly purified by column chromatography (SiO_2, MeOH in $CHCl_3$, 2–15%) to give a mixture (1.0 g, green oil) of **3l** and a fluorescent compound whose structure is unknown. This oil (0.41 g) was treated with (±)-DTT (0.69 g, 4.4 mmol) in DMF (7 mL) at room temperature for 0.5 h. $d^{fo}U$ (0.17 g, 0.68 mmol) was added to the solution, and the reaction mixture was stirred at room temperature for 0.5 h. $Sc(OTf)_3$ (34 mg, 0.070 mmol) and aqueous H_2O_2 (35%, 290 μL, 4.4 mmol) were added, and the mixture was stirred under O_2 at room temperature for 3 h. After removal of the solvent in vacuo, the residue was purified by flash column chromatography (neutral SiO_2, MeOH in $CHCl_3$, 0–6.5%) to give **4l** (54 mg, 0.14 mmol, 21%) as a green solid. The sample for elemental analysis and fluorescence experiments was obtained by crystallization from aq. EtOH as a green crystal (226 °C colored). UV: λ_{max} (ε, $M^{-1}cm^{-1}$) = 325 (18800) (aq. 100 mM HCl), 349 (12800) (10 mM phosphate buffer, pH 7.0), 346 (16100) (aq. 100 mM NaOH) nm. ^{1}H NMR (500 MHz, [D$_6$]DMSO): δ = 11.92 (s, 1 H, NH), 8.86 (s, 1 H, 6-H), 7.59 (d, J = 9.2 Hz, 1 H, 4′′-H), 7.04 (d, J = 2.3 Hz, 1 H, 7′′-H), 7.04 (dd, J = 8.6, 2.3 Hz, 1 H, 5′′-H), 6.19 (t, J = 6.3 Hz, 1 H, 1′-H), 5.35 (br. s, 2 H, NH_2), 5.31 (d, J = 4.0 Hz, 1 H, OH-3′), 5.04 (dd, J = 5.2, 4.6 Hz, 1 H, OH-5′), 4.28 (m, 1 H, 3′-H), 3.87 (m, 1 H, 4′-H), 3.61 (m, 2 H, 5′-H), 2.23 (m, 2 H, 2′-H) ppm. ^{13}C NMR (100 MHz, [D$_6$]DMSO): δ = 161.5, 152.9, 149.4, 146.6, 143.3, 139.2, 136.7, 122.3, 115.0, 107.7, 103.4, 87.8, 85.5, 70.4, 61.2, 40.3 ppm. ESI-MS (LR): m/z = 339 [M + Na]$^+$. $C_{16}H_{16}N_4O_5S{\cdot}3/5H_2O$: calcd. C 49.63, H 4.48, N 14.47, S 8.28; found C 49.88, H 4.48, N 14.10, S 8.52.

5-(5,6-Dimethoxybenzothiazol-2-yl)-5′-*O*-(4,4′-dimethoxytrityl)-2′-deoxyuridine (5): A solution of 5-(5,6-dimethoxybenzothiazol-2-yl)-2′-deoxyuridine (**4i**) (210 mg, 0.50 mmol) and DMTrCl (200 mg, 0.60 mmol) in pyridine (5 mL) was stirred at 40 °C for 5 h. After cooling of the mixture, the reaction was quenched by H_2O, and the solution was diluted with EtOAc (50 mL). The organic layer was washed with H_2O (50 mL × 2) and brine (40 mL), dried (Na_2SO_4), filtered, and concentrated in vacuo. The residue was purified by column chromatography (SiO_2, EtOAc in hexane 5–70%) to give **5** (270 mg, 0.37 mmol, 74%) as a yellow foam. ^{1}H NMR (400 MHz, $CDCl_3$): δ = 9.10 (s, 1 H, 6-H), 8.41 (br. s, 1 H, NH), 7.51–7.38 (m, total 6 H, DMTr), 7.23 (s, 1 H, 4′′-H or 7′′-H), 7.18–6.69 (m, total 7 H, DMTr), 6.49 (s, 1 H, 4′′-H or 7′′-H), 6.38 (t, J = 6.3 Hz, 1 H, 1′-H), 4.48 (m, 1 H, 3′-H), 4.07 (m, J = 3.2 Hz, 1 H, 4′-H), 3.93 (s, 3 H, benzothiazole-OCH_3), 3.69–3.65 (m, J = 10.9, 3.6 Hz, total 7 H, 5′a-H and DMTr-OCH_3 × 2), 3.54 (s, 3 H, benzothiazole-OCH_3), 3.36 (dd, J = 10.9, 3.2 Hz, 1 H, 5′b-H), 2.53 (ddd, J = 13.6, 5.9, 3.6 Hz, 1 H, 2′a-H), 2.41 (dt, J = 13.6, 6.8 Hz, 1 H, 2′b-H) ppm. ^{13}C NMR (125 MHz, [D$_6$]DMSO): δ = 161.4, 157.9, 156.6, 149.3, 148.7, 147.6, 145.8, 144.7, 138.9, 135.5, 135.5, 129.8, 129.7, 127.8, 127.7, 126.9, 126.6, 113.0, 107.5, 103.7, 103.0, 86.3, 86.1, 86.0, 70.3, 63.4, 55.9, 55.3, 54.8, 40.7 ppm. ESI-MS (LR): m/z = 746 [M + Na]$^+$. ESI-MS (HR): calcd. for $C_{39}H_{37}N_3O_9SNa$ 746.2143; found 746.2141.

3′-*O*-[2-Cyanoethoxy(*N*,*N*-diisopropylamino)phosphanyl]-5-(5,6-dimethoxybenzothiazol-2-yl)-5′-*O*-(4,4′-dimethoxytrityl)-2′-deoxyuridine (6): A solution of **5** (76 mg, 0.12 mmol), *N*,*N*-diisopropylethylamine (54 μL, 0.32 mmol), and 2-cyanoethyl *N*,*N*-diisopropylchlorophosphramidite (31 μL, 0.14 mmol) in CH_2Cl_2 (1 mL) was stirred at room temperature for 1 h. The reaction was quenched by H_2O, and the solution was diluted with $CHCl_3$ (20 mL). The organic layer was washed with saturated aqueous $NaHCO_3$ (20 mL) and brine (10 mL), dried (Na_2SO_4), filtered, and concentrated in vacuo. The residue was purified by column chromatography (neutral SiO_2, EtOAc in hexane 40–50%) to give **6** (77 mg, 84 μmol, 80%) as a pale yellow foam. ^{1}H NMR (500 MHz, $CDCl_3$): δ = 9.17, 9.13 (each s, each 0.5 H, 6-H), 8.34 (br. s, 1 H, NH), 7.53–7.38 (m, total 6 H, DMTr), 7.21, 7.21 (each s, each 0.5 H, 4′′-H or 7′′-H), 7.17–6.67 (m, total 7 H, DMTr), 6.38 (m, 1 H, 1′-H), 6.33, 6.29 (each s, each 0.5 H, 4′′-H or 7′′-H), 4.54 (m, 1 H, 3′-H), 4.22, 4.18 (each d, J = 2.9 Hz, each 0.5 H, 4′-H), 3.92, 3.92 (each s, total 3 H, benzothiazole-OCH_3), 3.79–3.54 {m, total 11 H, 5′a-H, OCH_2CH_2CN, DMTr-OCH_3 × 2, $N[CH(CH_3)_2]_2$}, 3.53, 3.52 (each s, each 1.5 H, benzothiazole-OCH_3), 3.30–3.27 (m, 1 H, 5′b-H), 2.62–2.39 (m, total 4 H, 2′-H, OCH_2CH_2CN), 1.16–1.01 {m, 12 H, $N[CH(CH_3)_2]_2$} ppm. ^{13}C NMR (100 MHz, $CDCl_3$): δ = 161.3, 161.2, 158.3, 155.7, 155.6, 149.4, 149.3, 148.6, 148.6, 147.7, 147.7, 146.3, 144.4, 138.9, 135.7, 135.6, 135.5, 135.4, 130.2, 130.2, 128.4, 128.3, 127.7, 126.7, 117.5, 117.3, 112.9, 112.9, 109.4, 109.3, 103.9, 101.6, 86.8, 86.8, 86.0, 77.2, 62.5, 58.3, 58.2, 58.0, 56.1, 55.6, 55.6, 55.0, 55.0, 43.2, 43.1, 43.1, 43.0, 40.8, 24.6, 24.5, 24.4, 24.4, 20.3, 20.3, 20.1, 20.0 ppm. ^{31}P NMR (202 MHz, $CDCl_3$): δ = 149.9, 149.2 ppm. ESI-MS (LR): m/z = 924 [M + H]$^+$. ESI-MS (HR): calcd. for $C_{48}H_{55}N_5O_{10}PS$ 924.3407; found 924.3400.

Oligonucleotide Synthesis: ODNs were synthesized with a DNA Synthesizer (Applied Biosystem Model 3400) by using $d^{bt}U$ phosphoramidite (**6**) and commercially available 2′-deoxyribonucleoside phosphoramidites at a 1-μmol scale following the standard procedure described. $d^{bt}U$ phosphoramidite (**6**) was used at a concentration of 0.12 M in dry MeCN, and the coupling time was extended to 15 min. After completion of the synthesis, the CPG support was treated with concentrated NH_4OH (55 °C, 12 h) and filtered off. The filtrate was concentrated, and the residue was dissolved in 0.1 M TEAA buffer (pH 7.0), which was placed on a Sep-pak C-18 column. Subsequently, the failure sequences without a 5′-DMTr group were washed out by 15% MeCN in 0.1 M TEAA buffer (pH 7.0), and the column was treated with aqueous 1% trifluoroacetic acid for 5 min at room temperature to remove the 5′-DMTr group of the ODN charged on the column. Further elution was carried out by H_2O and aqueous 50% MeCN to give the desired ODN. The solution was concentrated, and the residue was further purified on reversed-phase HPLC. HPLC conditions: column J'sphere ODS-M80 (4.6 × 150 mm, YMC); eluent A: 5% MeCN in 0.1 M

TEAA buffer (pH 7.0), B: 50% MeCN in 0.1 M TEAA buffer (pH 7.0); B conc. 10–30%/20 min; flow rate 1.0 mL/min.

Fluorescence Measurement: Fluorescence spectra were obtained at 25 °C in a 1-cm path length cell on a JASCO FP-750 spectrofluorometer. The fluorescence quantum yield (Φ) was determined by use of a quinine solution as a reference with a known Φ value of 0.53 in 0.1 M H_2SO_4.[19] The quantum yield was calculated according to the following equation:

$$\Phi_{SM} = \Phi_{ST} \frac{A_{SM}}{A_{ST}} \frac{I_{ST}}{I_{SM}} \frac{n_{SM}^2}{n_{ST}^2} \frac{F_{SM}}{F_{ST}}$$

A represents the optical density at the excitation wavelength, I represents the intensity of the excitation light, n represents the refractive index for the solvent, F represents the half width of the fluorescence spectrum. ST and SM represent the standard (quinine) and 5-(benzothiazol-2-yl)-2′-deoxyuridine derivatives (**4a**, **4c**–**l**) or ODNs containing d^{bt}U, respectively.

Enzymatic Digestion of ODNs: A mixture of ODN (0.5 OD_{260} units), SVPD (0.4 U), nuclease P1 (6×10^{-3} U), and calf intestine alkaline phosphatase (1.0 U) in acetate buffer (500 μL of a 0.2 M solution, pH 5.6) containing $ZnCl_2$ (10 mM) was incubated at 50 °C for 2 h. The mixture was then heated at 90 °C for 3 min. After removal of the enzymes with the Ultrafree®-Centrifugal Filter Unit (MILLIPORE), the filtrate was analyzed by reversed-phase HPLC. Each peak area was divided by ε_{260} (A, G, C and T) and ε_{350} (^{bt}U: 17100 $M^{-1}cm^{-1}$). HPLC conditions: column Capcell Pak C18 MG S-5 (250 × 4.6 mm, SHISEIDO); eluent A: 5% MeCN in 0.1 M TEAA buffer (pH 7.0), B: 80% MeCN in 0.1 M TEAA buffer (pH 7.0); B conc. 0–1%/10 min then 1–100%/10 min; flow rate 1.0 mL/min; column oven temp.: 40 °C.

CD Spectra of Modified and Unmodified DNA Duplexes: The CD spectra of the modified and unmodified DNA duplexes were recorded on a JASCO J-720 spectropolarimeter. The plots of molar ellipticity [θ] vs. wavelength [λ, nm] were obtained in phosphate buffer (10 mM, pH 7.0) containing NaCl (150 mM) at 25 °C. The blank experiments were also carried out under the same conditions. The concentration of each ODN was 3.0 μM. The measurements were carried out in a 0.1-cm path length cell. In a typical experiment, a solution of a duplex composed of two ODNs was heated to 90 °C for 3 min and allowed to cool to room temperature. The CD spectra of this solution were measured 8 times, integration over the range from 200 to 350 nm at 25 °C.

Computational Chemistry: All HOMO and LUMO calculations were performed at the HF/6-31G*(+) level by utilizing the Jaguar 7.7 programs released in 2010 (Jaguar version 7.7, Schrödinger, LLC, New York, NY, 2010). Geometries of the stacked methylated bases were constructed as follows. The corresponding dinucleotides were built up by using the Maestro 9.1 program released in 2010 (Maestro version 9.1, Schrödinger, LLC, New York, NY, 2010) with standard B-form DNA. All the sugar backbones of the dinucleotides were removed with the exception of the deoxyribose C1′ carbon and hydrogen atoms. Two hydrogen atoms were then attached to the C1′ methane atom to complete the stacked *N*-methylated bases. The ^{bt}Ura base was constructed, and the conformation was minimized by using the MacroModel 9.8 program released in 2010 (MacroModel version 9.8, Schrödinger, LLC, New York, NY, 2010). The MMFFs force field was used without considering the solvent effect. The initial structure was energy minimized, and the optimized structure was used as the starting structure for the next simulation. The local minimum was searched by the 5000-step energy minimization, and global minimum structures were searched by 1000 trials by using the MCMM option. The lowest-energy structure was re-minimized by DFT calculation [B3LYP/6-31G*(+)] in water by using the Jaguar 7.7 program, and the minimized structure was superimposed with one of the *N*-methylated bases in the dinucleotide models. The structures of the dinucleotide models containing ^{bt}Ura were used for the HOMO and LUMO calculations by single-point energy calculations.

Supporting Information (see footnote on the first page of this article): UV absorption and fluorescence spectra of compound **4a**, **4c**–**l**, sequences of the ODNs, enzymatic digestions of the ODNs, CD spectra of the mismatched duplexes, fluorescence spectra of the duplexes, quantum yields of the ODNs, HOMO and LUMO localization of the 5′-^{bt}UX-3′ and 5′-G^{bt}U-3′ containing protonated 5′-G, and ^{1}H, ^{13}C, and ^{31}P NMR spectra of the new compounds are presented.

Acknowledgments

This work was supported in part by Grant-in-Aid for Scientific Research from the Ministry of Education, Science, Sports and Culture of Japan. We thank Ms. M. Kiuchi, Ms. N. Saito, Ms. S. Oka, Ms. A. Tokumitsu, and Ms. A. Nagao (Center for Instrumental Analysis, Hokkaido University) for measurement of the elemental analysis and mass spectra.

[1] a) A. P. Breen, J. A. Murphy, *Free Radical Biol. Med.* **1995**, *18*, 1033–1077; b) M. Dizdaroglu, P. Jaruga, M. Birincioglu, H. Rodriguez, *Free Radical Biol. Med.* **2002**, *32*, 1102–1115; c) H. Kamiya, *Nucleic Acids Res.* **2003**, *31*, 517–531.
[2] J. Cadet, T. Delatour, T. Douki, D. Gasparutto, J.-P. Pouget, *Mutat. Res.* **1999**, *424*, 9–21.
[3] H. Kasai, *Mutat. Res.* **1997**, *387*, 147–163.
[4] a) S. Shibutani, M. Takeshita, *Nature* **1991**, *349*, 431–434; b) I. D. Donne, R. Rossi, R. Colombo, D. Giustarini, A. Milzani, *Clin. Chem.* **2006**, *52*, 601–623; c) R. P. Soultanakis, R. J. Melamede, I. A. Bespalov, S. S. Wallace, K. B. Beckman, B. N. Ames, D. J. Taatjes, M. W. Heininger, *Free Radical Biol. Med.* **2000**, *28*, 987–998; d) C.-C. Chiou, P.-Y. Chang, E.-C. Chan, T.-L. Wu, K.-C. Tsao, J. T. Wu, *Clin. Chim. Acta* **2003**, *334*, 87–94; e) L. Xue, M. M. Greenberg, *J. Am. Chem. Soc.* **2007**, *129*, 7010–7011; f) T. Nasr, Z. Li, O. Nakagawa, Y. Taniguchi, S. Ono, S. Sasaki, *Bioorg. Med. Chem. Lett.* **2009**, *19*, 727–730.
[5] H. Kasai, A. Iida, Z. Yamaizumi, S. Nishimura, H. Tanooka, *Mutat. Res.* **1990**, *243*, 249–253.
[6] A. Masaoka, H. Terato, M. Kobayashi, Y. Ohyama, H. Ide, *J. Biol. Chem.* **2001**, *276*, 16501–16510.
[7] Q.-M. Zhang, H. Sugiyama, I. Miyabe, S. Matsuda, I. Saito, S. Yonei, *Nucleic Acids Res.* **1997**, *25*, 3969–3973.
[8] a) A. Klungland, R. Paulsen, V. Rolseth, Y. Yamada, Y. Ueno, P. Wiik, A. Matsuda, E. Seeberg, S. Bjelland, *Toxicol. Lett.* **2001**, *119*, 71–78; b) H. Ånensen, F. Provan, A. T. Lian, S.-H. H. S. Reinertsen, Y. Ueno, P. Wiik, A. Matsuda, E. Seeberg, S. Bjelland, *Mutat. Res.* **2001**, *476*, 99–107.
[9] H. Kamiya, N. Murata-Kamiya, N. Karino, Y. Ueno, A. Matsuda, H. Kasai, *Mutat. Res.* **2002**, *513*, 213–222.
[10] a) T. Douki, T. Delatour, F. Paganon, J. Cadet, *Chem. Res. Toxicol.* **1996**, *9*, 1145–1151; b) T. Douki, T. Delatour, F. Bianchini, J. Cadet, *Carcinogenesis* **1996**, *17*, 347–353; c) S. Frelon, T. Douki, J.-L. Revanat, J.-P. Pouget, C. Tornabene, J. Cadet, *Chem. Res. Toxicol.* **2000**, *13*, 1002–1010; d) J. Cadet, T. Douki, S. Frelon, S. Sauvaigo, J.-P. Pouget, J.-L. Ravanat, *Free Radical Biol. Med.* **2002**, *33*, 441–449; e) J.-P. Pouget, S. Frelon, J.-L. Ravanat, I. Testard, F. Odin, J. Cadet, *Radiat. Res.* **2002**, *157*, 589–595; f) H. Hong, Y. Wang, *Anal. Chem.* **2007**, *79*, 322–326.
[11] H. A. Dahlmann, V. G. Vaidyanathan, S. J. Sturla, *Biochemistry* **2009**, *48*, 9347–9359.

[12] W. Hirose, K. Sato, A. Matsuda, *Angew. Chem. Int. Ed.* **2010**, *49*, 8392–8394.
[13] a) N. J. Greco, Y. Tor, *J. Am. Chem. Soc.* **2005**, *127*, 10784–10785; b) N. J. Greco, Y. Tor, *Tetrahedron* **2007**, *63*, 3515–3527.
[14] L. D. Lavis, R. T. Raines, *ACS Chem. Biol.* **2008**, *3*, 142–155.
[15] a) M. Torimura, S. Kurata, K. Yamada, T. Yokomaku, Y. Kamagata, T. Kanagawa, R. Kurane, *Anal. Sci.* **2001**, *17*, 155–160; b) M. Mizuta, K. Seio, A. Ohkubo, M. Sekine, *J. Phys. Chem. B* **2009**, *113*, 9562–9569; c) K. Fukui, K. Tanaka, M. Fujitsuka, A. Watanabe, O. Ito, *J. Photochem. Photobiol. B: Biology* **1999**, *50*, 18–27; d) F. D. Lewis, X. Liu, J. Liu, S. E. Miller, R. T. Hayes, M. R. Wasielewski, *Nature* **2000**, *406*, 51–53; e) F. D. Lewis, T. Wu, X. Liu, R. L. Letsinger, S. R. Greenfield, S. E. Miller, M. R. Wasielewski, *J. Am. Chem. Soc.* **2000**, *122*, 2889–2902; f) E. Zahavy, M. A. Fox, *J. Phys. Chem. B* **1999**, *103*, 9321–9327.
[16] a) M. J. Scanlan, I. H. Hillier, *J. Am. Chem. Soc.* **1984**, *106*, 3737–3745; b) P. Cieplak, P. Bash, U. C. Singh, P. A. Kollman, *J. Am. Chem. Soc.* **1987**, *109*, 6383–6289; c) A.-O. Colson, B. Besler, M. D. Sevilla, *J. Phys. Chem.* **1993**, *97*, 13852–13859; d) M. D. Sevilla, B. Besler, A.-O. Colson, *J. Phys. Chem.* **1995**, *99*, 1060–1063; e) M. Aida, K. Yamane, C. Nagata, *Mutat. Res.* **1986**, *173*, 49–54.
[17] a) I. Saito, M. Takayama, H. Sugiyama, K. Nakatani, *J. Am. Chem. Soc.* **1995**, *117*, 6406–6407; b) I. Saito, H. Sugiyama, *J. Am. Chem. Soc.* **1996**, *118*, 7063–7068; c) I. Saito, T. Nakamura, K. Nakatani, *J. Am. Chem. Soc.* **2000**, *122*, 3001–3006.
[18] M. L. Wilhelmsson, *Q. Rev. Biophys.* **2010**, *43*, 159–183.
[19] M. J. Adam, J. G. Highfield, G. F. Kirkbright, *Anal. Chem.* **1977**, *49*, 1850–1852.

Received: June 7, 2011
Published Online: August 30, 2011

